10.5665/SLEEP.1042

Tissue Vibration Induces Carotid Artery Endothelial Dysfunction: A Mechanism Linking Snoring and Carotid Atherosclerosis?

Jin-Gun Cho, MD[1,2]; Paul K. Witting, PhD[3]; Manisha Verma, BSc (Hons)[1]; Ben J. Wu, PhD[4]; Anu Shanu, MSc[3]; Kristina Kairaitis, MD, PhD[1,2]; Terence C. Amis, PhD[1,2]; John R. Wheatley, MD, PhD[1,2]

[1]Ludwig Engel Centre for Respiratory Research, Westmead Millennium Institute, Westmead, NSW, Australia; [2]Sydney Medical School, University of Sydney at Westmead Hospital, NSW, Australia; [3]Discipline of Pathology, Sydney Medical School, University of Sydney, NSW, Australia; [4]Heart Research Institute, Newtown, NSW, Australia.

Study Objectives: We have previously identified heavy snoring as an independent risk factor for carotid atherosclerosis. In order to explore the hypothesis that snoring-associated vibration of the carotid artery induces endothelial dysfunction (an established atherogenic precursor), we utilized an animal model to examine direct effects of peri-carotid tissue vibration on carotid artery endothelial function and structure.

Design: In supine anesthetized, ventilated rabbits, the right carotid artery (RCA) was directly exposed to vibrations for 6 h (peak frequency 60 Hz, energy matched to that of induced snoring in rabbits). Similarly instrumented unvibrated rabbits served as controls. Features of OSA such as hypoxemia, large intra-pleural swings and blood pressure volatility were prevented. Carotid endothelial function was then examined: (1) biochemically by measurement of tissue cyclic guanosine monophosphate (cGMP) to acetylcholine (ACh) and sodium nitroprusside (SNP); and (2) functionally by monitoring vessel relaxation with acetylcholine in a myobath.

Measurement and Results: Vessel cGMP after stimulation with ACh was reduced in vibrated RCA compared with unvibrated (control) arteries in a vibration energy dose-dependent manner. Vibrated RCA also showed decreased vasorelaxation to ACh compared with control arteries. Notably, after addition of SNP (nitric oxide donor), cGMP levels did not differ between vibrated and control arteries, thereby isolating vibration-induced dysfunction to the endothelium alone. This dysfunction occurred in the presence of a morphologically intact endothelium without increased apoptosis.

Conclusions: Carotid arteries subjected to 6 h of continuous peri-carotid tissue vibration displayed endothelial dysfunction, suggesting a direct plausible mechanism linking heavy snoring to the development of carotid atherosclerosis.

Keywords: Snoring, vibration, carotid atherosclerosis, endothelial dysfunction

Citation: Cho JG; Witting PK; Verma M; Wu BJ; Shanu A; Kairaitis K; Amis TC; Wheatley JR. Tissue vibration induces carotid artery endothelial dysfunction: a mechanism linking snoring and carotid atherosclerosis?. *SLEEP* 2011;34(6):751-757.

INTRODUCTION

A number of large epidemiological studies have shown a strong association between snoring and cerebral infarction.[1,2] However, in these studies, self-reported snoring was generally regarded as a surrogate for obstructive sleep apnea (OSA). Consequently, the focus for research into cerebrovascular sequelae of sleep-disordered breathing has centered on the pathophysiological consequences of acute obstructive events, including intermittent hypoxia and reoxygenation, hypercapnia, increased intrathoracic pressure swings, and cortical arousals. These physiological consequences may increase the risk of vascular disease via intermediary mechanisms including sympathetic activation, endothelial dysfunction, vascular oxidative stress, inflammatory pathways, hypercoagulable states, and metabolic dysregulation.[3,4] Presently, snoring vibrations per se as a risk factor for vascular disease has largely been ignored. Indeed, in the absence of coexisting OSA, the prevailing view of snoring is that there is little evidence to support a pathophysiological role in the promotion of vascular disease.[5,6]

A commentary on this article appears in this issue on page 693.

Submitted for publication September, 2010
Submitted in final revised form October, 2010
Accepted for publication December, 2010

Address correspondence to: Dr. Jin-Gun Cho, Ludwig Engel Centre for Respiratory Research, Department of Respiratory Medicine, Clinical Sciences Level 2, Westmead Hospital, P O Box 533, Wentworthville, NSW 2145, Australia; Tel: + 612 9845 6797; Fax: + 612 9845 7286. E-mail: jingun_cho@wmi.usyd.edu.au

However, we recently identified that heavy snoring in the absence of hypoxia is an independent risk factor for carotid atherosclerosis.[7] A mechanism to explain this finding was first proposed by Hedner and Sullivan, who noted that the close proximity of the carotid artery to the pharyngeal wall may expose the artery wall to vibration during snoring.[8] They hypothesized that during bouts of snoring, the carotid arteries would be subject to vibration energy levels that may induce carotid artery wall damage leading to atherosclerosis, a theory consistent with the "response-to-injury" model for atherogenesis.[9] Indeed we have previously shown that snoring associated vibrations are transmitted to the carotid artery wall in an animal model,[10,11] but it is not known whether these vibrations can result in carotid endothelial damage or dysfunction.

Endothelial dysfunction plays a pivotal role in the early pathogenesis of atherosclerosis.[12,13] It precedes the development of plaque, and is associated with vascular events related to atherosclerosis such as myocardial infarction.[14] Endothelial dysfunction (as measured by brachial artery flow-mediated dilatation)[15-17] has been demonstrated in patients with sleep-disordered breathing, but there is no established methodology for specific assessment of in vivo carotid artery endothelial function in humans. Therefore, we utilized a non-hypoxic, tracheostomized, anesthetized, rabbit model to examine whether delivery of a vibratory energy stimulus to the peri-carotid tissues (dosed matched to vibration energy levels occurring during snoring) was capable of inducing localized carotid artery endothelial dysfunction.

MATERIALS AND METHODS

A detailed description of the methods is provided in the supplemental material.

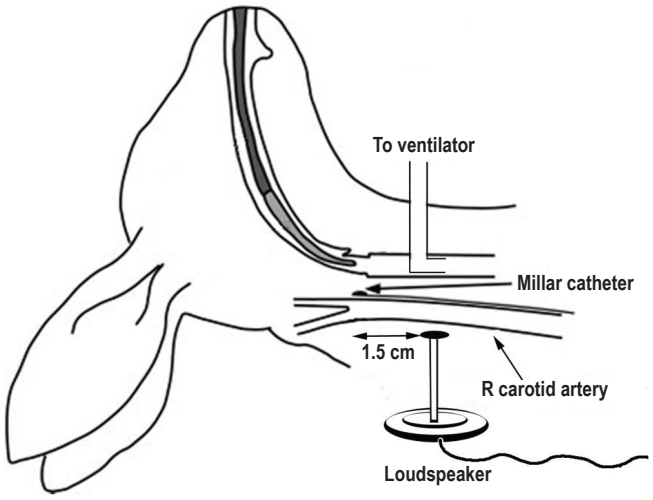

Figure 1—Schematic diagram of experimental setup. An anesthetized, supine rabbit was mechanically ventilated via tracheostomy. Pressure-transducer tipped catheters were surgically placed adjacent to the bifurcations of both right and left common carotid arteries. The flat circular tip (diameter 7.5 mm) of a plastic rod (10 cm length) attached to a loudspeaker (27 mm diameter) was placed on tissues overlying only the right carotid artery at a point 1.5 cm proximal to the right carotid artery bifurcation.

Animal Experiments

Studies were performed on 27 adult, male, anesthetized, New Zealand white rabbits (weight 3.41 ± 0.62 kg, mean ± SD). Protocols were approved by the Sydney West Area Health Service Animal Ethics Committee.

Anesthesia

Anesthesia was induced with intramuscular injection of ketamine (35 mg/kg) and xylazine (5 mg/kg) and maintained with a continuous intravenous infusion of ketamine (15 mg/kg/h) and xylazine (4.5/mg/kg/h). Bolus additions of sodium pentobarbitone (6.5 mg per bolus) were used to maintain apnea in order to minimize ventilator dys-synchrony. All animals were euthanized at the completion of each study using an overdose of intravenous sodium pentobarbitone.

Surgery

Animals were mechanically ventilated via surgical tracheostomy (Figure 1). Pressure transducer-tipped catheters (SPR-524, Millar Instruments, Houston, TX, USA) were surgically placed immediately adjacent to the left (LCA) and right carotid artery (RCA) bifurcations to quantify vibrations in the tissues surrounding the bifurcations. Arterial blood pressure was monitored during the study via an intra-aortic catheter (SPR-524).

Delivery of Vibration Energy

The flat circular tip (diameter 7.5 mm) of a 10-cm plastic rod attached to a loudspeaker was placed in contact with tissues overlying the RCA 1.5 cm caudal to the right carotid bifurcation (Figure 1). The speaker was attached to a signal generator producing square wave oscillations at 60 Hz frequency. Prior to commencement of each vibration exposure period, applied vibrations (< 5-sec duration) were used to adjust the amplitude of the oscillatory energy so that delivered tissue vibration energies detected by the RCA bifurcation catheter were targeted to vibration energy levels (~170×10^{-4} [cm H_2O]^2) previously reported for induced snoring in rabbits.[10]

Monitoring Physiological Parameters

Temperature, pulse, oxygen saturation, and end-tidal CO_2 ($ETCO_2$) were continuously monitored. When required, supplemental oxygen ensured normoxia throughout the study and peak $ETCO_2$ was maintained at 5% to 6%. Data were digitized (4 kHz sampling rate for pressure transducer tipped catheter signals, 0.1 to 4 kHz for all other data signals) via a Powerlab 16/30 data acquisition unit (ADInstruments, Sydney, Australia) and recorded using signal acquisition software (LabChart 7, ADInstruments).

Experimental Protocol

Following surgery, the RCA was exposed to continuous direct mechanical vibration for 6 hours. Seventeen rabbits were exposed to the vibration stimulus, while the remaining 10 rabbits constituted an unvibrated sham operated control group. For each control rabbit, both the LCA and RCA were used as separate control specimens. After euthanasia, intravascular perfusion[18] with either formaldehyde or saline was performed depending on the specific requirements for the subsequent arterial specimen study. Both the LCA and RCA were then carefully excised. Where possible, carotid arteries were divided into 2 samples of equal length, which allowed utilization for both biochemical and functional studies.

Calculation of Vibration Energy

Data were analyzed in the frequency domain using the signal acquisition software's power spectral function. A fast Fourier transform algorithm (2,048-point fast Fourier transform size, Hann window with 50% overlap) was performed on the tissue pressure signal data from the transducer tipped catheters at both the right and left carotid bifurcations across the entire 6-h study. Vibration energy was calculated by integrating power over the 50 Hz-1 kHz frequency bandwidth as previously described.[10]

Absorbance Spectroscopy Studies

Absorbance spectroscopy studies were performed on 7 vibrated RCA (vRCA) samples, 7 LCA samples from vibrated rabbits (vLCA) and 8 control carotid samples from unvibrated rabbits. Samples were homogenized and determinations of arterial cGMP with and without ACh stimulation (1 μM) were performed as previously described using a commercial ELISA kit and absorbance spectroscopy[19] after normalization to total homogenate protein.[20] Separately, 5 vRCA, 5 vLCA, and 6 control samples were treated with 1 μM sodium nitroprusside, homogenized, and assayed for cGMP as above as a positive control.

Vascular Reactivity Studies

Vascular reactivity studies were performed on 5 vRCA, 5 vLCA, and 5 control carotid samples. Isometric tension was recorded with a force transducer connected to a data acquisition unit (Powerlab 8/30 and Octal Bridge Amplifier, ADInstruments), and ACh concentration-response curves were generated as described previously.[19]

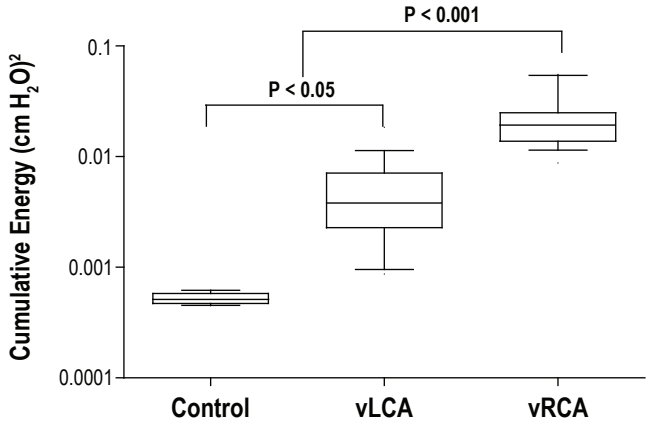

Figure 2—Six-hour median delivered vibration energy from 50-1000 Hz bandwidth calculated from power spectral analysis of signals from pressure transducer-tipped catheters. Data plotted using a log scale. Control = unvibrated carotids; vRCA = directly vibrated right carotid arteries; vLCA = indirectly vibrated left carotid arteries. Horizontal line = median values; box = interquartile range, bars = 10th to 90th centile range. Energy at vRCA was significantly greater than that at both vLCA and control arteries, while energy at vLCA was greater than control background energy.

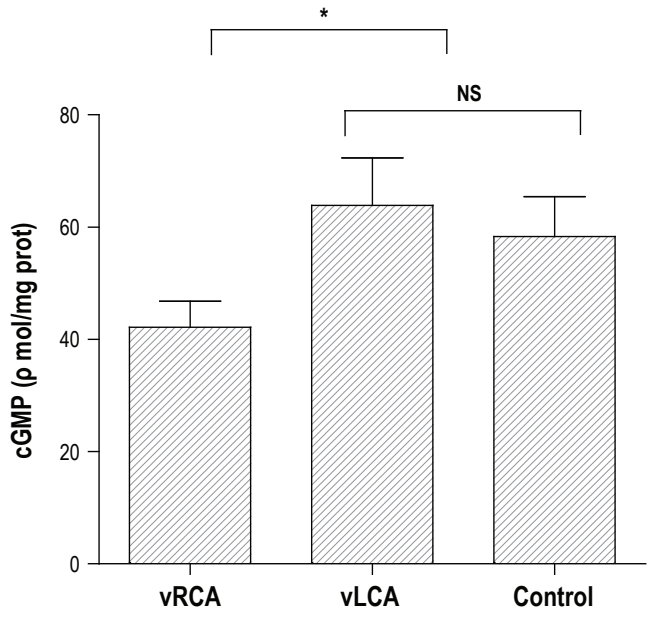

Figure 3—Tissue cGMP was measured in directly vibrated RCA (vRCA), indirectly vibrated LCA (vLCA) and unvibrated carotid arteries (control) after exposure to 1 μM acetylcholine using a commercial kit. Data represent mean values +1 SD. Note that the cGMP content within vRCA was significantly less than that for control and vLCA but there was no dfference between vLCA and control arteries. (* P < 0.05).

Endothelial Cell Viability Studies

Viability studies were performed using 3 vRCA, 2 vLCA, and 2 control carotid samples. Immunohistochemistry with smooth muscle actin identified smooth muscle cells and carotid endothelium under light microscopy. Cellular apoptosis was determined using the TUNEL method, and hydrated sections were prepared and stained[21] using a commercial kit (Millipore, Temecula, CA, USA). A thymus section from an unvibrated rabbit served as a positive control in view of its increased cellular turnover. Light microscopy slides were scanned, digitized, and images were analyzed (Imagescope software Version 10, Aperio), and the number of positive stained pixels (brown) as a percentage of the total pixels was determined (Positive Pixel Count Algorithm version 9, Aperio).[22]

Apoptosis was also independently quantified by measuring the activity of effector caspases 3 and 7 using Caspase-Glo 3/7 Assay (Promega, Southampton, UK) according to the manufacturer's protocol in homogenates obtained from vRCA, vLCA, and control carotid samples (n = 4 all groups) with luminescence results expressed as relative light units (RLU) as described.[23]

Statistical Analysis

Data were expressed as mean ± SD or median and interquartile range as appropriate. For cGMP and caspase analyses, matched artery (i.e., within rabbit) comparisons were performed using a paired Student *t*-test while unmatched (i.e., between rabbits) comparisons were performed using a 2-sample *t*-test. Bonferroni corrections were applied for multiple comparisons. cGMP versus cumulative vibration energy relationships were examined via linear regression. Vascular relaxation curves were fitted with exponential 2 phase association functions for between curve comparisons, or repeated measures ANOVA between groups (control, vRCA, vLCA) and ACh level followed by testing for significant differences at each ACh level using either 2-sample *t*-tests (control vs vRCA; control vs vLCA) or paired *t*-tests (vRCA vs vLCA). Statistical analyses were performed using the Prism 5 statistical program (GraphPad, San Diego, CA, USA) and SPSS version 16.0 (SPSS Inc, Chicago, IL, USA). $P < 0.05$ was considered significant.

RESULTS

Delivered Vibration Energy

In the studies where the RCA was vibrated (vRCA, n = 17), the median 95% cumulative tissue vibration energy measured at the RCA was 192×10^{-4} (cm H_2O)^2, similar to the median value of 170×10^{-4} (cm H_2O)^2 previously reported during induced snoring in rabbits (Figure 2).[10] Tissue vibrations were also detected at the LCA in vibrated rabbits (vLCA; n = 17) but at a significantly lower energy level (38×10^{-4} [cm H_2O]^2; $P < 0.001$ compared with vRCA). There were significantly higher delivered tissue vibration energy levels for both the vRCA and vLCA when compared with values recorded for unvibrated control arteries (5×10^{-4} [cm H_2O]^2; n = 10; both $P < 0.001$).

Tissue Cyclic Guanosine Monophosphate (cGMP)

Baseline values for tissue cGMP tended to be lower in the vRCA samples (13.6 ± 4.8 ρmol/mg; n = 6) compared with vLCA (18.2 ± 4.6 ρmol/mg; n = 4) and control artery samples (18.5 ± 3.2 ρmol/mg; n = 7), but this difference failed to reach statistical significance ($P = 0.11$). However, following the addition of ACh, cGMP was significantly lower in vRCA samples (42.1 ± 4.6 ρmol/mg; n = 7) compared with both control arteries (58.3 ± 7.1 ρmol/mg; n = 5) and vLCA (63.9 ± 8.5 ρmol/mg; n = 7; all $P < 0.01$; Figure 3). With the addition of 1 μM sodi-

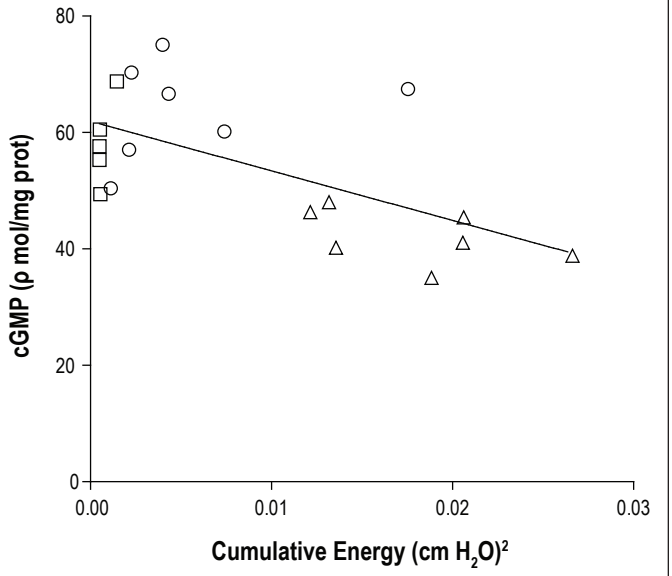

Figure 4—cGMP for carotid arteries after the addition of ACh, plotted against cumulative vibration energy, for individual unvibrated carotid arteries (squares), indirectly vibrated LCA (circles), and directly vibrated RCA (triangles). Note the inverse linear relationship between cGMP and increasing vibration energy (solid line; $r^2 = 0.38$; $P < 0.01$).

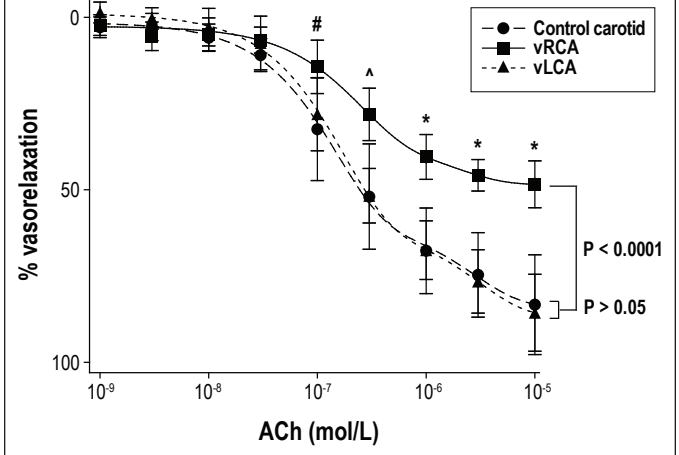

Figure 5—Vascular relaxation curves plotted as percent reduction in initial tension with increasing ACh concentration for vibrated RCA (squares; n = 5), vibrated LCA (triangles; n = 5) and control carotid arteries (circles; n = 5). Data were fitted by exponential 2-phase association functions (all $r^2 > 0.92$). Data are mean values; bars represent ± 1 SD. Note the reduced vascular relaxation for vibrated RCA compared with indirectly vibrated LCA and control carotid arteries at the same concentration of ACh. (#P < 0.05 vRCA vs vLCA/control; ^P < 0.02 vRCA vs vLCA/control; *P < 0.01 vRCA vs vLCA/control; *t*-tests).

um nitroprusside, there was no significant difference in cGMP between vRCA samples (73.2 ± 10.6 ρmol/mg; n = 5), vLCA (77.8 ± 7.2 ρmol/mg; n = 5) and control arteries (71.8 ± 7.1 ρmol/mg; n = 7; P = 0.5).

There was a significant inverse linear relationship between measured tissue vibration energy dose and post ACh cGMP levels for vRCA, vLCA, and control carotid arteries ($r^2 = 0.38$; $P < 0.01$; Figure 4) equivalent to a 6.8% fall in cGMP per 50×10^{-4} (cm H_2O)^2 increase in tissue vibration energy.

Vascular Reactivity

vRCA segments demonstrated reduced vascular relaxation compared with vLCA segments and with control carotid artery segments at ACh concentrations above 10^{-7} mol/L (all $P < 0.05$; all groups n = 5; Figure 5). When the data were fitted with an exponential 2-phase association function (all $r^2 > 0.92$), a significant reduction in vascular relaxation to ACh in vRCA compared with both the vLCA and control carotid arteries was evident ($P < 0.0001$, F test; Figure 5). However, there was no significant difference in vascular relaxation between the vLCA and control carotid arteries at any concentration of ACh ($P > 0.6$).

Viability Assays

Under light microscopy, arterial endothelial cell integrity was preserved in both vRCA (n = 3) and control carotid artery samples (n = 2) with no evidence of endothelial denudation, disruption to the endothelial layer, or damage to the arterial smooth muscle cells (see Figure S1 in the supplemental material). Assessment of caspase-3/7 activity did not reveal any difference between vRCA (1021 ± 44 RLU), vLCA (1020 ± 35 RLU), or control carotid arteries (1030 ± 48 RLU; all groups n = 4; P = 0.95). In addition, assessment of TUNEL staining (quantified by positive pixel counting) demonstrated that vRCA values (3.42% ± 0.59% positive pixels; n = 3) were similar to vLCA and control samples (2.50% ± 1.39% positive pixels; n = 4 combined; P = 0.34), whereas values were much greater in the thymus control sample (7.3% positive pixels) [See Figure S2 in the supplemental material for TUNEL stains].

DISCUSSION

This study demonstrates that a single 6-hour period of carotid artery wall vibration, at a dose-rate matched to previously measured snoring in anesthetized rabbits, resulted in endothelial dysfunction as evidenced by: (1) dose-related vibration energy reductions in cGMP response to ACh; and (2) impaired carotid artery vasorelaxation to ACh. Furthermore, an intact endothelium and absence of increased apoptosis in vibrated carotid arteries excluded gross morphological damage as a cause of the vascular dysfunction.[12] These findings demonstrate vibration-induced endothelial dysfunction, providing a plausible pathophysiological mechanism linking snoring and localized carotid atherosclerosis.

This is the first study to specifically measure carotid artery endothelial function in response to peri-carotid tissue vibration. It is important to note that the study was not intended to test the effect of snoring per se, but to probe the concept that even small, physiologically relevant vibrations can result in significant carotid artery endothelial dysfunction. In contrast to studies of high-intensity vibrations on peripheral arteries in models of vibration-induced white finger,[24-26] our study is the first model to specifically examine the effect of physiologically relevant vibrations, dose matched to induced snoring in rabbits,[10] on carotid arterial endothelial function.

The quantification of arterial tissue cGMP[27,28] and assessment of vasorelaxation to ACh[29,30] are validated measures of arterial nitric oxide bioavailability and markers of vascular function.[13,31] The vasorelaxation response to ACh has been used to ascertain vascular function in human arteries[28] as well as in

rabbit arteries.[29] Specifically, impairments in cGMP response and vasorelaxation to ACh are recognized as demonstrating arterial endothelial dysfunction.[31]

Our findings of a reduction in tissue cGMP response to ACh of vibrated carotid arteries and functional impairment in vasorelaxation (compared to controls) support the presence of endothelial dysfunction in vibrated carotid arteries. ACh induces vasorelaxation via an endothelial-dependent pathway[32] through activation of endothelial nitric oxide synthase (eNOS) which in turn generates nitric oxide. Nitric oxide enters the vascular smooth muscle and converts GTP to cGMP, which results in vasorelaxation.[32] In contrast, the absence of difference in the cGMP response of vibrated and non-vibrated carotid arteries to stimulation with sodium nitroprusside[27] (an endothelium-independent source of nitric oxide) demonstrates that the underlying smooth muscle was unaffected by vibrations, and localizes the vascular dysfunction solely to the endothelium.

Measured tissue cGMP and functional arterial vasorelaxation within left carotid arteries (which were subjected to lower levels of vibration energy) and unvibrated carotid arteries were not different. However, small amplitude vibrations were detected in the left carotid artery, implying that there may be a threshold effect for vibration energy induced endothelial dysfunction. If translated into snoring intensity, this suggests that lower intensity, or soft snoring has less potential for carotid endothelial dysfunction than loud or heavy snoring. This concept is supported by the significant inverse dose-response relationship between the amount of vibration energy detected in the peri-carotid tissues and carotid artery cGMP levels, with lower cGMP levels in arteries subjected to higher vibration energies.

In contrast to previous high intensity ("jackhammer model") vascular vibration studies in rats' tails, which have resulted in significant endothelial cell vacuolation and denudation of the endothelium,[24] our endothelial viability investigations (immunohistochemistry, TUNEL, and caspase studies) showed no morphological cellular damage or increased apoptosis compared with control arteries, thus eliminating gross structural damage of cells as a cause of reduced cGMP and impaired vasorelaxation. The vascular significance of this is its consistency with the established "response-to-injury" model of atherosclerosis in which initial injurious events do not necessarily lead to endothelial denudation or morphological damage, but still result in endothelial dysfunction and eventually, early atherosclerotic lesions.[9,12,33]

Heavy snoring has been postulated to have pathogenic effects on other peri-pharyngeal tissues. There is evidence of mucosal sensory nerve damage in OSA subjects,[34,35] and histological evidence of inflammatory changes within the upper airway mucosa and muscles,[36-40] which have been attributed to trauma from snoring vibration and recurrent upper airway closure. Snoring vibrations can be detected distal to the upper airway mucosal tissues, in a rabbit model.[10,11] Indeed, these models demonstrated amplification of energy within the carotid artery lumen for frequencies in the 75 to 275 Hz bandwidth,[10] possibly to be due to carotid artery wall resonance.[11] Therefore, our results showing endothelial dysfunction from carotid vibration support the notion that heavy snoring vibrations in themselves cannot be considered a benign entity, and have the potential to exert pathogenic effects on the carotid endothelium.

The finding that small vibrations (with equivalent energy to that of snores) result in carotid endothelial dysfunction has crucial vascular implications. Endothelial dysfunction precedes the development of atherosclerosis,[41] and is strongly associated with other vascular risk factors such as diabetes[31,42] and smoking.[43] Brachial artery endothelial dysfunction has been demonstrated in subjects with obstructive sleep apnea[17,44] and, is improved following continuous positive airway pressure (CPAP).[44,45] Other factors such as obesity, hypertension, hyperlipidemia, and hyperglycemia will contribute to endothelial dysfunction in these subjects; however, there has been very little investigation of the potential pathogenic role of snoring vibrations in the development of carotid artery disease, despite the clear association of heavy snoring with a higher prevalence of stroke in the population.[1,2,46,47]

This hypothesis was explored in a recent observational study from our laboratory involving the association between heavy snoring and carotid atherosclerosis in adults.[7] Heavy snoring (occurring for more than 50% of the night) was significantly associated with carotid atherosclerosis, after adjustment for cardiovascular risk factors. Importantly, this association was not seen for the femoral artery, suggestive of a site-specific effect of snoring localized to the carotid artery. The present study now suggests a plausible underlying mechanism for this finding.

Although we have tested for the presence of endothelial dysfunction by measuring the secondary messenger cGMP in carotid arterial tissue, and via endothelial-dependent vasorelaxation studies, we have not explored the biochemical pathways by which this dysfunction occurs. Reduced NO bioavailability may be due to decreased expression of eNOS,[48] a reduction in cofactors and substrates that regulate eNOS,[49] inappropriate activation of eNOS through alterations of cellular signalling,[50] or an increased degradation of NO via reaction of superoxide anion, forming peroxynitrite[51] which can itself inhibit soluble guanylate cyclase activity[52,53] and mediate direct oxidative injury to the endothelium.[54,55] One potential pathway was demonstrated in vibrated rat digital arteries showing reduced NO activity with an increase in the reactive oxygen species, hydrogen peroxide (H_2O_2), suggestive of eNOS uncoupling leading to diminished NO production.[56]

The applied vibration frequency (60 Hz) was selected since it lies within the reported dominant frequency bandwidth (68 ± 15 Hz) of airflow oscillations for human snoring, including snores recorded from OSA patients,[57] and has also been used in previous animal studies of vibration induced vascular damage and tissue inflammation[24-26,58] and vibration transmission from the upper airway.[11] Vibrations were applied continuously for 6 hours instead of intermittently as occurs in snoring. However, it is likely that the total snoring vibration energy intermittently transmitted on a nightly basis for many years would substantially outweigh the effect of only 6 hours of continuous vibration energy. We also applied direct external vibration of the right carotid artery rather than internally via the airway as in previous studies.[11,58] This method was chosen because it would not have been possible to simultaneously deliver airway vibrations, mechanically ventilate the animal for 6 hours, and create a stable operative environment including the elimination of hypoxemia, hypercapnia, and enhanced intra-pleural pressure swings. Indeed, the stable physiological environment was one of the main strengths of our study design, which effectively eliminated potential confounders related to alterations in gas exchange and

enhanced negative pleural pressure levels seen in obstructive sleep apnea. The validity of our results were strengthened by the use of left carotid arteries in vibrated rabbits as an internal control artery, as these arteries were subjected to the same physiological environment apart from vibration intensity.

In this study we have demonstrated significant endothelial dysfunction in carotid arteries after a single period of vibration but many questions remain unanswered. These include the role of vibration amplitude, different vibration frequencies, the pathogenic effect of snoring vibrations to the carotid artery every night for many years, as well as its interaction with other vascular risk factors. In addition, continuous versus intermittent vibrations may affect endothelial function differently. Finally, an important area of future research would involve examining the potential impact of vibrations in promoting rupture of existing carotid atherosclerotic plaques, leading to distal cerebral emboli and acute cerebrovascular events. However, this study and our previous demonstration of an independent association of heavy snoring and carotid atherosclerosis[7] highlight the importance of snoring vibrations in the absence of hypoxia as a pathogenic mechanism in the development of carotid endothelial dysfunction and atherosclerosis.[8]

CONCLUSION

Peri-carotid tissue vibrations at an energy matched for rabbit snores during a single 6-hour period resulted in reduced carotid artery cGMP production and NO-dependent vasorelaxation consistent with endothelial dysfunction, which is associated with the development of atherosclerosis. We speculate that snoring energy transmitted to carotid artery walls and leading to endothelial dysfunction may promote the development of early carotid atherosclerosis in heavy snorers. A clearer understanding of the mechanisms by which snoring-like vibrations lead to carotid endothelial dysfunction may suggest new therapeutic and preventative strategies aimed at reducing the risk of carotid atherosclerosis and stroke in heavy snorers.

ABBREVIATIONS

OSA, obstructive sleep apnea
RCA, right carotid artery
cGMP, cyclic guanosine monophosphate
ACh, acetylcholine
SNP, sodium nitroprusside
SD, standard deviation
LCA, left carotid artery
$ETCO_2$, end tidal carbon dioxide
Hz, hertz
vRCA, directly vibrated right carotid artery
vLCA, left carotid artery from vibrated rabbits
TUNEL, terminal deoxynucleotidyl transferase nick end labelling
RLU, relative light units
ANOVA, analysis of variance
cm H_2O, centimeters of water
CPAP, continuous positive airway pressure
eNOS, endothelial nitric oxide synthase,
GTP, guanosine triphosphate
NO, nitric oxide
ELISA, enzyme-linked immunosorbent assay

ACKNOWLEDGMENTS

The authors would like to thank Dr. Karen Byth for her support in the statistical analyses. This work was supported by grants from the National Health and Medical Research Council of Australia (Project Grant 570789) and Australian Research Council (DP0878559). Dr. Cho is the recipient of a University of Sydney Postgraduate Award (co-funded), a McCaughey Research Entry Scholarship (Royal Australasian College of Physicians) and is supported by the Westmead Medical Research Foundation.

DISCLOSURE STATEMENT

This was not an industry supported study. Dr. Amis has consulted for Glaxo Smith Kline. Dr. Wheatley has consulted for Actelion, Apnex Medical, Boehringer Ingelheim, and Glaxo Smith Kline. The other authors have indicated no financial conflicts of interest.

REFERENCES

1. Koskenvuo M, Kaprio J, Telakivi T, Partinen M, Heikkilä K, Sarna S. Snoring as a risk factor for ischaemic heart disease and stroke in men. Br Med J (Clin Res Ed) 1987;294:16-9.
2. Hu F, Willet W, Manson J, et al. Snoring and the risk of cardiovascular disease in women. J Am Coll Cardiol 2000;35:308-13.
3. Shamsuzzaman AS, Gersh BJ, Somers VK. Obstructive sleep apnea: implications for cardiac and vascular disease. JAMA 2003;290:1906-14.
4. Caples SM, Garcia-Touchard A, Somers VK. Sleep-disordered breathing and cardiovascular risk. Sleep 2007;30:291-303.
5. Waller PC, Bhopal RS. Is snoring a cause of vascular disease? An epidemiological review. Lancet 1989;333:143-6.
6. Hoffstein V. Is snoring dangerous to your health? Sleep 1996;19:506-16.
7. Lee SA, Amis TC, Byth K, et al. Heavy snoring as a cause of carotid artery atherosclerosis. Sleep 2008;31:1207-13.
8. Hedner JA, Wilcox I, Sullivan CE. Speculations on the interaction between vascular disease and obstructive sleep apnea. In: Saunders NA, Sullivan CE, eds. Sleep and breathing. New York: Marcel Dekker, 1994.
9. Ross R. Atherosclerosis – an inflammatory disease. N Engl J Med 1999;340:115-26.
10. Amatoury J, Howitt L, Wheatley JR, Avolio AP, Amis TC. Snoring-related energy transmission to the carotid artery in rabbits. J Appl Physiol 2006;100:1547-53.
11. Howitt L, Kairaitis K, Kirkness JP, et al. Oscillatory pressure wave transmission from the upper airway to the carotid artery. J Appl Physiol 2007;103:1622-7.
12. Ross R. The pathogenesis of atherosclerosis: a perspective for the 1990s. Nature 1993;362:801-9.
13. Stocker R, Keaney JF Jr. Role of oxidative modifications in atherosclerosis. Physiol Rev 2004;84:1381-478.
14. Davignon J, Ganz P. Role of endothelial dysfunction in atherosclerosis. Circulation 2004;109[suppl III]:III-28-32.
15. Kato M, Roberts-Thomson P, Phillips BG, et al. Impairment of endothelium-dependent vasodilation of resistance vessels in patients with obstructive sleep apnea. Circulation 2000;102:2607-10.
16. Carlson JT, Rangemark C, Hedner JA. Attenuated endothelium-dependent vascular relaxation in patients with sleep apnoea. J Hypertens 1996;14:577-84.
17. Ip MS, Tse HF, Lam B, Tsang KW, Lam WK. Endothelial function in obstructive sleep apnea and response to treatment. Am J Respir Crit Care Med 2004;169:348-53.
18. Tulis DA. Histological and morphometric analyses for rat carotid balloon injury model. In: Sreejayan N, Totowa RJ, eds. Methods in molecular medicine, Vol 139: Vascular biology protocols. NJ: Humana Press, 2007.
19. Witting PK, Rayner BS, Wu BJ, Ellis NA, Stocker R. Hydrogen peroxide promotes endothelial dysfunction by stimulating multiple sources of superoxide anion radical production and decreasing nitric oxide bioavailability. Cell Physiol Biochem 2007;20:255-68.
20. Smith PK, Krohn RI, Hermanson GT, et al. Measurement of protein using bicinchoninic acid. Anal Biochem 1985;150:76-85.

21. Gavrieli Y, Sherman Y, Ben-Sasson SA. Identification of programmed cell death in situ via specific labeling of nuclear DNA fragmentation. J Cell Biol 1992;119:493-501.
22. Garcia L, Bermudez V, Brett M, Peroza L, Landa J, Borregales F. Quantitative analytical technique applied to histopathology of birds infected experimentally by the virus of chicken anemia virus. Diagn Pathol 2008;3 Suppl 1:S21.
23. Liu D, Li C, Chen Y, et al. Nuclear import of proinflammatory transcription factors is required for massive liver apoptosis induced by bacterial lipopolysaccharide. J Biol Chem 2004;279:48434-42.
24. Curry BD, Govindaraju SR, Bain JL, et al. Evidence for frequency-dependent arterial damage in vibrated rat tails. Anat Rec A Discov Mol Cell Evol Biol 2005;284:511-21.
25. Curry BD, Bain JL, Yan J, et al. Vibration injury damages arterial endothelial cells. Muscle Nerve 2002;25:527-34.
26. Govindaraju SR, Bain JL, Eddinger TJ, Riley DA. Vibration causes acute vascular injury in a two-step process: vasoconstriction and vacuole disruption. Anat Rec 2008;291:999-1006.
27. Huang A, Thomas SR, Keaney JF Jr. Measurements of redox control of nitric oxide bioavailability. Methods Enzymol 2002;359:209-16.
28. Schulz E, Tsilimingas N, Rinze R, et al. Functional and biochemical analysis of endothelial (dys)function and NO/cGMP signaling in human blood vessels with and without nitroglycerin pretreatment. Circulation 2002;105:1170-5.
29. Thomas SR, Schulz E, Keaney JF Jr. Hydrogen peroxide restrains endothelium-derived nitric oxide bioactivity--role for iron-dependent oxidative stress. Free Radic Biol Med 2006;41:681-8.
30. Furchgott RF, Zawadzki JV. The obligatory role of endothelial cells in the relaxation of arterial smooth muscle by acetylcholine. Nature 1980;288:373-6.
31. Koltai MZ, Hadhazy, P, Posa I, et al. Characteristics of coronary endothelial dysfunction in experimental diabetes. Cardiovasc Res 1997; 34:157-63.
32. Murad F. Cyclic guanosine monophosphate as a mediator of vasodilation. J Clin Invest 1986;78:1-5.
33. Ross R. The pathogenesis of atherosclerosis – an update. N Engl J Med 1986;314:488-500.
34. Friberg D, Gazelius B, Lindblad LE, Nordlander B. Habitual snorers and sleep apnoics have abnormal vascular reactions of the soft palate mucosa on afferent nerve stimulation. Laryngoscope 1998;108:431-6.
35. Kimoff RJ, Sforza E, Champagne V, Ofiara L, Gendron D. Upper airway sensation in snoring and obstructive sleep apnea. Am J Respir Crit Care Med 2001;164:250-5.
36. Friberg D, Ansved T, Borg K, Carlsson-Nordlander B, Larsson H, Svanborg E. Histological indications of a progressive snorers disease in an upper airway muscle. Am J Respir Crit Care Med 1998;157:586-93.
37. Sekosan M, Zakkar M, Wenig BL, Olopade CO, Rubinstein I. Inflammation in the uvula mucosa of patients with obstructive sleep apnea. Laryngoscope 1996;106:1018-20.
38. Woodson BT, Garancis JC, Toohill RJ. Histopathologic changes in snoring and obstructive sleep apnea syndrome. Laryngoscope 1991;101(12 Pt 1):1318-22.
39. Paulsen FP, Steven P, Tsokos M, et al. Upper airway epithelial structural changes in obstructive sleep-disordered breathing. Am J Respir Crit Care Med 2002;166:501-9.
40. Boyd JH, Petrof BJ, Hamid Q, Fraser R, Kimoff RJ. Upper airway muscle inflammation and denervation changes in obstructive sleep apnea. Am J Respir Crit Care Med 2004;170:541-6.
41. Shimokawa H. Primary endothelial dysfunction: atherosclerosis. J Mol Cell Cardiol 1999;31:23-37.
42. Hogikyan RV, Galecki AT, Pitt B, Halter JB, Greene DA, Supiano MA. 1998 Specific impairment of endothelium-dependent vasodilation in subjects with type 2 diabetes independent of obesity. J Clin Endocrinol Metab 1998;83:1946-52.
43. Celermajer DS, Sorensen KE, Georgakopoulos D, et al. Cigarette smoking is associated with dose-related and potentially reversible impairment of endothelium-dependent dilation in healthy young adults. Circulation 1993;88(5 Pt 1):2149-55.
44. Lattimore JL, Wilcox I, Skilton M, Langenfeld M, Celermajer DS. Treatment of obstructive sleep apnoea leads to improved microvascular endothelial function in the systemic circulation. Thorax 2006;61:491-5.
45. Imadojemu VA, Gleeson K, Quraishi S, Kunselman AR, Sinoway LI, Leuenberger UA. Impaired vasodilator responses in obstructive sleep apnea are improved with continuous positive airway pressure therapy. Am J Respir Crit Care Med 2002;165:950-3.
46. Partinen M, Palomaki H. Snoring and cerebral infarction. Lancet 1985;2:1325-6.
47. Arzt M, Young T, Finn L, Skatrud J, Bradley T. Association of sleep disordered breathing and the occurrence of stroke. Am J Respir Crit Care Med 2005;172:1447-51.
48. Wilcox JN, Subramanian RR, Sundell CL, et al. Expression of multiple isoforms of nitric oxide synthase in normal and atherosclerotic vessels. Arterioscler Thromb Vasc Biol 1997;17:2479-88.
49. Pou S, Pou WS, Bredt DS, Snyder SH, Rosen GM. Generation of superoxide by purified brain nitric oxide synthase. J Biol Chem 1992;267:24173-6.
50. Shimokawa H, Flavahan NA, Vanhoutte PM. Loss of endothelial pertussis toxin-sensitive G protein function in atherosclerotic porcine coronary arteries. Circulation 1991;83:652-60.
51. Harrison DG. Endothelial function and oxidant stress. Clin Cardiol 1997;20(11 Suppl 2):II-11-7.
52. Rubanyi GM, Vanhoutte PM. Superoxide anions and hyperoxia inactivate endothelium—derived relaxing factor. Am J Physiol Heart Circ Physiol 1986;250:H222-7.
53. Munzel T, Daiber A, Ullrich V, Mülsch A. Vascular consequences of endothelial nitric oxide synthase uncoupling for the activity and expression of the soluble guanylyl cyclase and the cGMP-dependent protein kinase. Arterioscler Thomb Vasc Biol 2005;25:1551-7.
54. Gryglewski RJ, Palmer RM, Moncada S. Superoxide anion is involved in the breakdown of endothelium-derived vascular relaxing factor. Nature 1986;320:454-6.
55. Moncada S, Higgs A. The L-arginine-nitric oxide pathway. N Engl J Med 1993;329:2002-12.
56. Hughes JM, Wirth O, Krajnak K, et al. Increased oxidant activity mediates vascular dysfunction in vibration injury. J Pharmacol Exp Ther 2009;328:223-30.
57. Liistro G, Stanescu DC, Veriter C, Rodenstein DO, Aubert Tulkens G. Pattern of snoring in obstructive sleep apnea patients and in heavy snorers. Sleep 1991;14:517-25.
58. Almendros I, Acerbi I, Puig F, Montserrat JM, Navajas D, Farré R. Upper-airway inflammation triggered by vibration in a rat model of snoring. Sleep 2007;30:225-7.

MATERIALS AND METHODS (IN DETAIL)

Studies were performed on 27 adult, male, anesthetised, New Zealand white rabbits (weight 3.41 ± 0.62 kg, mean ± SD). All protocols were approved by the Sydney West Area Health Service Animal Ethics Committee.

Anesthesia

Anesthesia was induced with intramuscular injection of ketamine (35 mg/kg) and xylazine (5 mg/kg) and maintained with a continuous intravenous infusion of ketamine (15 mg/kg/h) and xylazine (4.5 mg/kg/h). Bolus additions of sodium pentobarbitone (6.5 mg per bolus) were used to maintain apnoea in order to minimise ventilator dys-synchrony. All animals were euthanized at the completion of each study using an overdose of intravenous sodium pentobarbitone.

Surgery

Studies were performed in the supine position with rabbits initially breathing spontaneously. A ventral neck skin incision was used to expose the cervical trachea and a tracheostomy cannula was inserted into the caudal tracheal lumen through an incision made between the 3rd and 4th tracheal cartilage (Figure S1). The cannula, connected to an in-line pneumotachograph (8300A, Hans Rudolf, Kansas City, MO, USA) used to monitor inspiratory/expiratory airflow, was attached to a pressure-cycled ventilator (Infant Star, Infrasonics Inc., San Diego, CA, USA) allowing the animal to be mechanically ventilated (tidal volume: 20-25 mL; respiratory rate: 50-60 breaths/min; peak inspiratory pressure: 8-10 cm H_2O; inspiratory to expiratory time ratio: 1:1.5). Both left and right common carotid arteries were identified via careful blunt dissection. The right femoral artery was surgically exposed in the mid thigh region and under direct vision a pressure transducer tipped catheter (SPR-524, Millar Instruments, Houston, TX, USA) was introduced into the femoral artery lumen and then advanced into the abdominal aorta to monitor blood pressure. The catheter was sutured in place with the femoral artery ligated distally.

Two pressure transducer-tipped catheters (Millar SPR-524) were placed in the tissues immediately adjacent to the left and right common carotid artery walls and positioned with the sensor at the carotid bifurcation (angle of the mandible). These catheters were used to quantify vibrations in the tissues surrounding the carotid artery bifurcation. Correct positioning and orientation of both transducers was verified at postmortem examination.

Delivery of Vibration Energy

The flat circular tip (diameter 7.5 mm) of a 10-cm plastic rod attached to a 27-mm diameter loudspeaker (C2208, Dick Smith Electronics, Australia) was placed in contact with the tissues overlying the right common carotid artery (RCA) at a point 1.5 cm caudal to the right carotid bifurcation (Figure S1). The speaker was attached to a signal generator (BWD 160A Function Generator, BWD Electronics, Melbourne, Australia) that produced square wave oscillations at a 60 Hz frequency. Prior to commencement of each vibration exposure study period, short periods of applied vibration (< 5 sec) were used to adjust the amplitude of the oscillatory excitation signal so that delivered tissue vibration energies, as detected by the right carotid artery bifurcation catheter, were targeted to vibration energy levels ($\sim 170 \times 10^{-4}$ [cm H_2O]^2) previously reported from our laboratory for induced snoring in rabbits.[1]

Monitoring Physiological Parameters

Core body temperature was continuously monitored with a rectal probe (YSI 400 series, Yellow Springs Instrument Co., Yellow Springs, OH, USA), while a 3 lead ECG was used to record heart rate and rhythm. Oxygen saturation was measured by pulse oximetry (Ohmeda Biox 3700e, Ohmeda, Boulder, CO, USA) with the probe placed on the left thigh, and with supplemental oxygen added to ensure normoxia throughout the study. End-tidal CO_2 ($ETCO_2$) was measured with a carbon dioxide analyser (Exerstress CO21, Sydney, Australia). Ventilatory parameters were adjusted to maintain peak $ETCO_2$ at 5% to 6%. Data were digitized (4 KHz sampling rate for pressure transducer tipped catheter signals, 0.1 to 4 KHz for all other data signals) via a Powerlab 16/30 data acquisition unit (ADInstruments, Sydney, Australia) and recorded using signal acquisition software (LabChart 7, ADInstruments).

Experimental Protocol

Following surgery, the RCA was exposed to continuous direct mechanical vibration for a period of 6 hours. Seventeen rabbits were exposed to the vibration stimulus, while the remaining 10 rabbits constituted an unvibrated sham operated control group. For each control rabbit, both the left carotid artery (LCA) and RCA were used as separate control specimens. At the end of the study period, animals were euthanized, a thoracotomy was performed, and the ascending aorta cannulated. Intravascular perfusion, at physiological pressure levels, was used to flush out the rabbit's entire blood volume with either 10% v/v neutral buffered formaldehyde for immunohistochemistry studies (n = 4) or Dulbecco's phosphate buffered saline for absorbance spectroscopy, caspase assay and vascular reactivity studies (n = 23).[2] An incision made in the left atrium allowed an outlet for blood and perfused fluid. After total intravascular perfusion, both LCA and RCA were carefully excised and extraneous tissue adherent to the carotid arteries was removed via dissection. Where possible, carotid arteries were divided into 2 equal length samples, thus allowing a single excised artery to be utilized for both biochemical and functional studies.

Calculation of Vibration Energy

Data were analysed in the frequency domain using the signal acquisition software's power spectral function. A fast Fourier transform algorithm (2,048-point fast Fourier transform size, Hann window with 50% overlap) was performed on the tissue pressure signal data from the transducer tipped catheters at both the right and left carotid bifurcations across the entire 6-h study. Vibration energy was calculated by integrating power over the 50 Hz-1 kHz frequency bandwidth as previously described.[1]

Absorbance Spectroscopy Studies

Absorbance spectroscopy studies were performed on 7 vibrated RCA (vRCA) samples, 7 LCA samples from vibrated rabbits (vLCA) and 8 control carotid artery samples from unvibrated rabbits. Samples were homogenized using a rotating piston and matching Teflon-lined tube as described previously.[3]

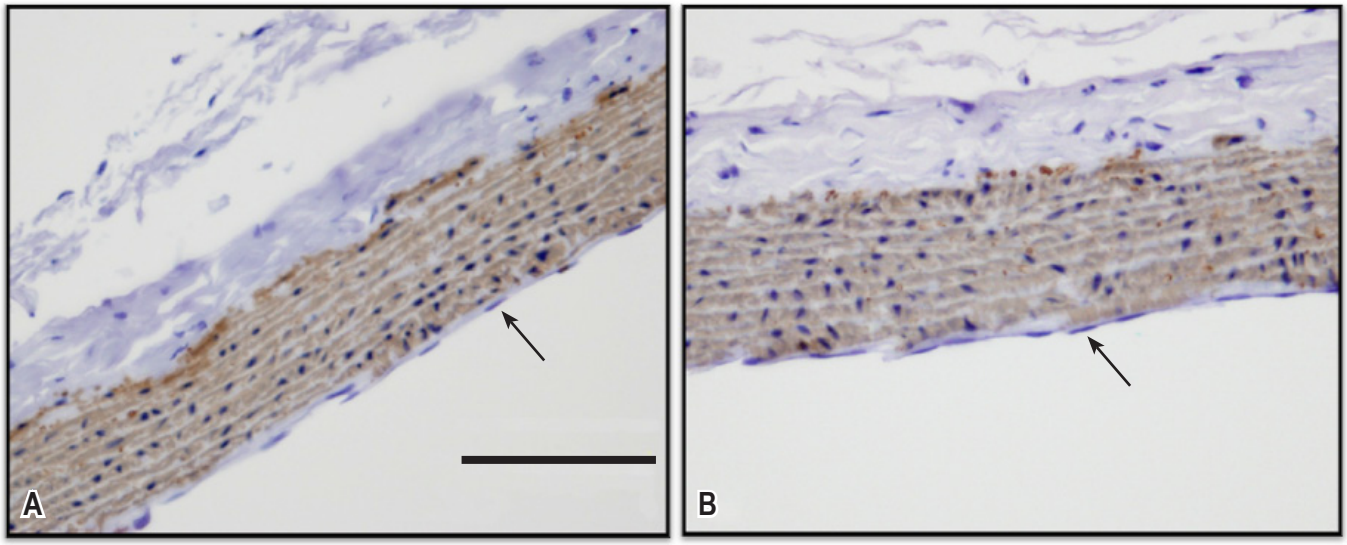

Figure S1—Representative arterial sections stained with a smooth muscle actin antibody and viewed under light microscopy. Images obtained from a vibrated right carotid artery (**A**) and control carotid artery (**B**). No differences were seen between the vibrated and control arteries in the vascular smooth muscle (brown stain) or in the endothelial layer (arrows indicate the endothelium as a monolayer on the internal aortic surface). Bar = 100 μm for both panels.

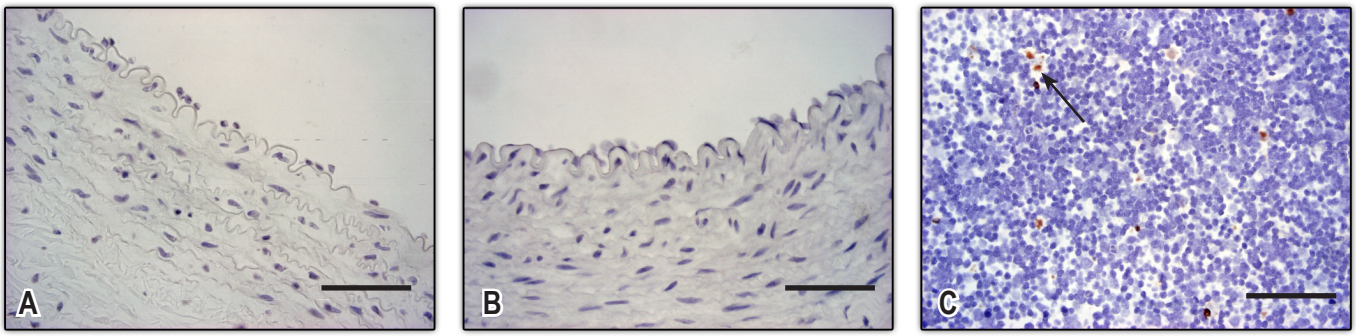

Figure S2—Light microscopy of representative sections with TUNEL staining of: (**A**) vibrated RCA; (**B**) unvibrated (control) carotid artery; and (**C**) a segment of thymus. Cells undergoing apoptosis stain brown. Apoptotic cells are also seen within the thymus (**C**; black arrow). Note the lack of positive TUNEL staining in either vibrated (**A**) or control carotid arteries (**B**). Bar = 50 μm for all sections.

Determinations of arterial cGMP with and without ACh stimulation (1 μM) in the presence of 100 μM *L*arginine and 200 μM 3-isobutyl-1-methylxanthine (IBMX) were performed using a commercial kit (Cayman Chemical, Ann Arbor, MI, USA). Absorbance spectroscopy was performed using a multi-well plate reader (Victor[3], Perkin Elmer, Waltham, MA, USA). Separately, 5 vRCA, 5 vLCA, and 6 control samples were treated with 1 μM sodium nitroprusside (SNP) for 30 minutes, added to an IBMX-containing buffer and homogenized and assayed for cGMP as above. All cGMP data were normalized to total homogenate protein using the bicinchoninic acid protein assay[4] and finally expressed in units as ρmol per mg of protein.

Vascular Reactivity Studies

Vascular reactivity studies were performed on 5 vRCA, 5 vLCA, and 5 control carotid artery samples that were perfused in 50 mM phosphate buffered saline (vehicle control) at 4°C for 1 h, cut into 3-mm ring segments and then mounted, via 2 metal pins passed through the lumen, in a double-jacketed tissue myobath system (World Precision Instruments, Inc., Sarasota, FL, USA). The rings were bathed in 20 mL of modified Krebs-Henseleit solution (in mM: 11 D-glucose, 1.2 $MgSO_4$, 12 KH_2PO_4, 4.7 KCl, 120 NaCl, 25 $NaHCO_3$, and 2.5 $CaCl_2 \cdot 2H_2O$) at 37ºC and aerated with 5% CO_2.[3] Isometric mechanical tension was recorded with a force transducer connected to a data acquisition unit (Powerlab 8/30 and Octal Bridge Amplifier, ADInstruments). After mounting, the rings were stretched to a resting tension of 2 g. Next, during a 30-min equilibration period, the segments were washed once with modified Krebs-Henseleit solution, then contracted with 0.1 mM phenylephrine (Phe), following which the response to consecutive addition of ACh (10^{-9}-10^{-5} mol/L) was monitored.[3] The % relaxation was calculated based on 100% contraction to 0.1 mM Phe, and ACh concentration-response curves were then generated.

Endothelial Cell Viability Studies

Viability studies were performed using 3 vRCA, 2 vLCA, and 2 control artery samples. Carotid artery sample sections were fixed in 10% v/v neutral buffered formaldehyde and em-

bedded in paraffin, mounted onto superfrost slides, baked at 60°C for 1 hour, cleared in xylene, and hydrated through a descending alcohol series to distilled water. Immunohistochemistry was performed to image smooth muscle actin in order to identify the smooth muscle cells and carotid endothelium under light microscopy. Endothelial cell apoptosis was determined using the terminal deoxynucleotidyl transferase (dUTP) nick end labeling (TUNEL) method, and hydrated sections were prepared and stained essentially as described by Gavrieli et al.[5] using an ApopTag Peroxidase In Situ Apoptosis Detection Kit (Millipore, Temecula, CA, USA). In view of the increased cellular turnover and apoptosis present in the thymus, a thymus section from an unvibrated rabbit served as a positive control. Light microscopy slides were scanned and digitised using a digital slide scanner (Scanscope CS system, Aperio Technologies, Vista, CA, USA) at magnification x40 with a resolution of 25 μm/pixel. The digital images were analysed (Imagescope software Version 10, Aperio), and the number of positive stained pixels (brown) as a percentage of the total (positive plus negative) pixels was determined (Positive Pixel Count Algorithm version 9, Aperio).

Apoptosis was also independently quantified by measuring the activity of effector caspases 3 and 7 using Caspase-Glo 3/7 Assay (Promega, Southampton, UK) in homogenates obtained from vRCA, vLCA, and control artery samples (n = 4 all groups) with luminescence results expressed as relative light units (RLU).

Chemicals

Chemicals were of the highest possible grade. ACh, *L*arginine, SNP, and Krebs-Henseleit powder were from Sigma (Australia). All buffers were prepared with Millipore Water and stored at 4°C prior to use.

Statistical Analysis

Data were expressed as mean ± SD or median and interquartile range as appropriate. Vibration energy data were log transformed to approximate normality prior to analysis. Matched artery (i.e., within rabbit) comparisons were performed using a paired Student *t*-test while unmatched (i.e., between rabbits) comparisons were performed using a 2-sample *t*-test with Bonferroni corrections for multiple comparisons. The relationship between cGMP and cumulative vibration energy was examined via linear regression. Vascular relaxation curves were fitted with exponential two phase association functions followed by an extra sum-of-squares F test for between curve comparisons, or repeated measures ANOVA between groups and ACh level followed by testing for significant differences at each ACh level using either 2-sample *t*-tests (control vs vRCA; control vs vLCA) or paired *t*-tests (vRCA vs vLCA). Statistical analyses were performed using the Prism 5 statistical program (GraphPad, San Diego, CA, USA) and SPSS version 16.0 (SPSS Inc, Chicago, IL, USA). $P < 0.05$ was considered significant.

REFERENCES

1. Amatoury J, Howitt L, Wheatley JR, Avolio AP, Amis TC. Snoring-related energy transmission to the carotid artery in rabbits. J Appl Physiol 2006;100:1547-53.
2. Tulis DA. Histological and morphometric analyses for rat carotid balloon injury model. In: Sreejayan N, Totowa RJ, eds. Methods in molecular medicine, Vol 139: Vascular biology protocols. NJ: Humana Press, 2007.
3. Witting PK, Rayner BS, Wu BJ, Ellis NA, Stocker R. Hydrogen peroxide promotes endothelial dysfunction by stimulating multiple sources of superoxide anion radical production and decreasing nitric oxide bioavailability. Cell Physiol Biochem 2007;20:255-68.
4. Smith PK, Krohn RI, Hermanson GT, et al. Measurement of protein using bicinchoninic acid. Anal Biochem 1985;**150**:76-85.
5. Gavrieli Y, Sherman Y, Ben-Sasson SA. Identification of programmed cell death in situ via specific labeling of nuclear DNA fragmentation. J Cell Biol 1992;119:493-501.